Eur. Phys. J. A **20**, 397–404 (2004)
DOI 10.1140/epja/i2003-10168-1

THE EUROPEAN PHYSICAL JOURNAL A

On the magnitude of single-particle proton and neutron separation energies in the chains of isotopes and isotones near closed shells

V.I. Isakov[1,a], K.A. Mezilev[1], K.I. Erokhina[2], B. Fogelberg[3], H. Mach[3], and E. Ramström[3]

[1] Petersburg Nuclear Physics Institute, Russian Academy of Sciences, Gatchina 188300, Russia
[2] Physical Technical Institute, Russian Academy of Sciences, St. Petersburg 194021, Russia
[3] Department of Radiation Sciences, Uppsala University, Nyköping S-61162, Sweden

Received: 18 November 2003 /
Published online: 26 May 2004 –
Communicated by V.V. Anisovich

Abstract. Single-particle separation energies of protons or neutrons in nuclei near the closed shells are examined in the chains of isotopes or isotones. From the observed dependences we determine spins and parities of the single-particle orbitals and their sequence in nuclei far from the stability line, where direct experimental information on single-particle characteristics is not available at present.

PACS. 21.10.Dr Binding energies and masses – 21.60.Cs Shell model – 21.10.Pc Single-particle levels and strength functions

1 Introduction

Nucleon separation energies $B_{n=\pi,\nu}$ are the main structure indicators which define the borders of stability of nuclei against nucleon decay in the regions far from the stability line. In this sense they determine the global characteristics of nuclei. The difference between B_π and B_ν for the neighbouring isobars represents the energy released in the β-decay ($Q_{\beta^-}(Z,N) = B_\pi(Z+1,N-1) - B_\nu(Z,N) + m_\nu - m_\pi - m_e$), thus providing information on the rate of this process which is one of the main modes of nuclear decay. At the same time these parameters may also reveal peculiarities of nuclear structure. This has a direct impact on the spherical nuclei near the closed shells where the spherical shell structure and related symmetries manifest themselves in the most profound way. This aspect of the study of single-particle separation energies is investigated in the present paper.

2 General considerations

Our aim is to study the changes in the neutron (proton) separation energies in the chain of isotones (isotopes) caused by a successive addition of protons (neutrons) to the nuclei. For the illustration of our line of arguments let us consider the Hartree-Fock method where the single-particle energies ε_i are defined as

$$\varepsilon_i \;=\; \langle i|\hat{T}|i\rangle \;+\; \sum_{k(\varepsilon_k<\varepsilon_{\rm F})} {}_a\langle ik|\hat{\vartheta}|ik\rangle_a \;, \qquad (1)$$

and where by neglecting the rearrangement effects, the single-particle separation energies become $B^i = -\varepsilon_i$ (Koopmans' theorem [1]). Then the variation of the separation energy of the valence nucleon "i" (neutron or proton) caused by an addition to the system of nucleons of the other type, which occupy the orbitals "p" ($\varepsilon_p > \varepsilon_{\rm F}$), may be given as

$$\delta B^i \;=\; -\sum_{p(\varepsilon_p>\varepsilon_{\rm F})} {}_a\langle ip|\hat{\vartheta}|ip\rangle_a \;, \qquad (2)$$

where $\varepsilon_{\rm F}$ refers to the initial nucleus. Thus, in this approach the variation of the binding energy (*i.e.* the separation energy) of the valence nucleon equals the potential energy of its interaction with the added nucleons of the other type taken with the opposite sign. If we remove nucleons from the orbits p', the corresponding variation of the binding energy is

$$\delta B^i \;=\; +\sum_{p'(\varepsilon_{p'}<\varepsilon_{\rm F})} {}_a\langle ip'|\hat{\vartheta}|ip'\rangle_a \;, \qquad (3)$$

where the sum over p' refers to the removed nucleons, while $\varepsilon_{\rm F}$ also refers to the initial nucleus.

[a] e-mail: visakov@thd.pnpi.spb.ru

Formulae (2) and (3) are written schematically, whereas in the realistic case we must specify the coupling scheme and corresponding quantum numbers for the description of multiparticle wave functions. To this aim we select multiparticle states formed of the groups of nucleons $\{j^n; s, J\}$, where each group contains n particles ($0 \le n \le 2j+1$; for the filled orbit we have $n = 2j+1$) and it is characterized by the seniority quantum number s (additional quantum numbers α are possible) and the total angular momentum J of the group. For the lowest states of nuclei we have $s = J = 0$ for even n, while for odd n the seniority quantum number $s = 1$ and $J = j$. An additional complication arises if we consider separation energy in odd-odd nuclei. In this case we have to specify the total nuclear spin I arising from the total spins of the proton $\{j_\pi\}$ and neutron $\{j_\nu\}$ valence groups, $|j_\nu - j_\pi| \le I \le j_\nu + j_\pi$, perform the calculations for all components of the proton-neutron multiplet and select the state with spin I corresponding to the lowest energy. Thus, to determine the separation energies we should calculate the energy of the proton-neutron interaction between the groups of protons and neutrons, each built in the jj-coupling scheme and characterized by the s, α and J quantum numbers.

3 Multiparticle matrix elements of the interaction

We consider two groups of nucleons $\{j_1^{n_1}; s_1, J_1\}$ and $\{j_2^{n_2}; s_2, J_2\}$, which have the total spin I, and calculate the total interaction energy between these groups. Actually we are interested in the case when $j_1 \in \pi$ and $j_2 \in \nu$ (or vice versa). The corresponding matrix element is

$$M\,(j_1^{n_1} s_1 J_1, j_2^{n_2} s_2 J_2; I) \equiv$$

$$\left\langle j_1^{n_1} s_1 J_1, j_2^{n_2} s_2 J_2; I \middle| \sum_{i,k} \hat{\vartheta}(ik) \middle| j_1^{n_1} s_1 J_1, j_2^{n_2} s_2 J_2; I \right\rangle . \quad (4)$$

Here the index "i" refers to the group $\{j_1^{n_1}\}$, while the index "k" refers to the group $\{j_2^{n_2}\}$. By using fractional parentage expansions [2,3] for antisymmetrical states in the jj-coupling scheme,

$$|j_1^{n_1} s_1 J_1\rangle \;=$$

$$\sum_{J_{01} s_{01}} \langle j_1^{n_1} s_1 J_1 | \} j_1^{n_1-1} s_{01} J_{01}, j_1\rangle |j_1^{n_1-1} s_{01} J_{01}, j_1; J_1\rangle \quad (5)$$

and

$$|j_2^{n_2} s_2 J_2\rangle \;=$$

$$\sum_{J_{02} s_{02}} \langle j_2^{n_2} s_2 J_2 | \} j_2^{n_2-1} s_{02} J_{02}, j_2\rangle |j_2^{n_2-1} s_{02} J_{02}, j_2; J_2\rangle, \quad (6)$$

we obtain the matrix element (4) in the form

$$\begin{aligned} M\,(j_1^{n_1} s_1 J_1, j_2^{n_2} s_2 J_2; I) &= n_1 n_2 (2J_1+1)(2J_2+1) \\ &\times \sum_{s_{01} s_{02} J_{01} J_{02} L J} (2L+1)(2J+1) \begin{Bmatrix} J_{01} & j_1 & J_1 \\ J_{02} & j_2 & J_2 \\ L & J & I \end{Bmatrix}^2 \\ &\times \langle j_1^{n_1} s_1 J_1 | \} j_1^{n_1-1} s_{01} J_{01}, j_1\rangle^2 \\ &\times \langle j_2^{n_2} s_2 J_2 | \} j_2^{n_2-1} s_{02} J_{02}, j_2\rangle^2 \cdot V_J^{\text{p-p}}(j_1 j_2) \;, \end{aligned} \quad (7)$$

where $V_J^{\text{p-p}}(j_1 j_2) = \langle j_1 j_2 J | \hat{\vartheta}(1,2) | j_1 j_2 J\rangle$ is the particle-particle matrix element of the interaction with the total angular momentum of the pair J. Note that, though in our case $\{j_1\}$ and $\{j_2\}$ refer to different types of nucleons by taking into account the charge-exchange components of nuclear forces ($\sim \boldsymbol{\tau}_1 \cdot \boldsymbol{\tau}_2$), we must also calculate the matrix element V_J between the antisymmetrized states of the proton-neutron pair. Consider the case where n_1 is odd ($s_1 = 1$, $J_1 = j_1$ in such case), while n_2 is even ($s_2 = J_2 = 0$). Then for fractional parentage coefficients entering formula (7) we have the expressions

$$\langle j_2^{n_2} s_2 = 0 \; J_2 = 0 | \} j_2^{n_2-1} s_{02} = 1 \; J_{02} = j_2, j_2\rangle^2 \;=\; 1 \quad (8)$$

and

$$\begin{aligned} \langle j_1^{n_1} s_1 = 1 \, J_1 = j_1 | \} j_1^{n_1-1} s_{01} J_{01}, j_1\rangle^2 \;=\; & \\ & \frac{(2j_1 - n_1)}{n_1(2j_1-1)}\, \delta(J_{01}, 0) \\ & + \frac{2(n_1-1)(2J_{01}+1)}{n_1(2j_1-1)(2j_1+1)} \, \frac{\left[1 + (-1)^{J_{01}}\right]}{2} \;, \end{aligned} \quad (9)$$

where in (9) $s_{01} = 0$ if $J_{01} = 0$, while $s_{01} = 2$ if $J_{01} \ne 0$; J_{01} is even.

As a result, after some algebraic transformations, the matrix element (4) takes the form

$$\begin{aligned} M\left(j_1^{n_1\,\text{odd}} s_1 = 1 \, J_1 = j_1, j_2^{n_2\,\text{even}} s_2 = 0 \, J_2 = 0; I = j_1\right) = & \\ \frac{n_1 n_2}{(2j_1+1)(2j_2+1)} \sum_J (2J+1) V_J^{\text{p-p}}(j_1 j_2) \;. \end{aligned} \quad (10)$$

The expression for the matrix element (4) is more complicated in the case when both n_1 and n_2 are odd. To write it in a more solid form we introduce auxiliary symbols as follows:

$$\begin{aligned} v_1^2 &= \frac{(n_1-1)}{(2j_1-1)} \,, \qquad v_2^2 = \frac{(n_2-1)}{(2j_2-1)} \,, \\ u_1^2 &= 1 - v_1^2 = \frac{(2j_1 - n_1)}{(2j_1-1)} \,, \\ u_2^2 &= 1 - v_2^2 = \frac{(2j_2 - n_2)}{(2j_2-1)} \;. \end{aligned} \quad (11)$$

After certain transformations we obtain the result

$$M\left(j_1^{n_1\,\mathrm{odd}} s_1=1\, J_1=j_1, j_2^{n_2\,\mathrm{odd}} s_2=1\; J_2=j_2; I\right) = \left[v_1^2(u_2^2-v_2^2)\frac{1}{(2j_2+1)}+v_2^2(u_1^2-v_1^2)\frac{1}{(2j_1+1)}+v_1^2v_2^2\right] \times\sum_J(2J+1)\,V_J^{\text{p-p}}(j_1j_2)\;+\left(v_1^2v_2^2+u_1^2u_2^2\right)V_I^{\text{p-p}}(j_1j_2) +\left(v_1^2u_2^2+u_1^2v_2^2\right)V_I^{\text{p-h}}(j_1j_2)\;. \quad (12)$$

Here

$$V_I^{\text{p-h}}(j_1j_2) \;=\; -\sum_J(2J+1)\begin{Bmatrix} j_1 j_2 I \\ j_1 j_2 J\end{Bmatrix}V_J^{\text{p-p}}(j_1j_2) \quad (13)$$

represents the expansion of the particle-hole matrix element in terms of the particle-particle ones (Pandya relationship [4]). Note that the u and v terms as defined by (11) are the analogs of the u, v coefficients in the Bogoliubov transformation and by the appearance they coincide with those obtained in the approach of isolated j-level, with the inclusion of the blocking effect.

In the special case of $j = 1/2$ and $n = 1$ formula (11) would be undetermined. However, it follows from the derivation of (12), that in this case one should substitute $(2j-n)/(2j-1)\to 1$ and $(n-1)/(2j-1)\to 0$.

In the case of both n_1 and n_2 even ($s_1 = s_2 = J_1 = J_2 = 0$), the expression for the matrix element M (formula (4)) has also the form (10), but both n_1 and n_2 are now even there. Note that multiparticle matrix elements involved in the nuclear-structure calculations were also considered in ref. [5]. In the present work we calculate the separation energy of the valence nucleon (proton or neutron) by the subsequent filling of the free orbitals (or by removing corresponding particles from the filled orbitals), in accordance with the selected single-particle scheme. Thus, for this evaluation we only need the matrix elements (10) and (12) with $n_1 = s_1 = 1$.

4 Selection of the interaction

There are two ways to define the matrix elements $V_J^{\text{p-p}}(j_1j_2)$ and $V_J^{\text{p-h}}(j_1j_2)$ that enter formulae (10) and (12). The first way is to calculate them using an effective interaction like the effective forces that we have successfully employed, in the framework of the RPA method, to describe different properties of nuclei close to ^{208}Pb, ^{132}Sn and ^{100}Sn [6–10], where the corresponding experimental information is available. This interaction, which we label here as the "standard" one, was also used to study the properties of hypothetical nuclei in the vicinity of ^{164}Pb [11] as well as for the calculation of the mass surface profile in nuclei close to ^{78}Ni [12]. It has the form

$$\widehat{\vartheta}(1,2)=\exp\left(-\frac{r_{12}^2}{r_0^2}\right)\cdot\Big(V+V_\sigma\widehat{\boldsymbol{\sigma}}_1\widehat{\boldsymbol{\sigma}}_2+V_T\widehat{S}_{12} +V_\tau\widehat{\boldsymbol{\tau}}_1\widehat{\boldsymbol{\tau}}_2+V_{\tau\sigma}\widehat{\boldsymbol{\sigma}}_1\widehat{\boldsymbol{\sigma}}_2\cdot\widehat{\boldsymbol{\tau}}_1\widehat{\boldsymbol{\tau}}_2+V_{\tau T}\widehat{S}_{12}\widehat{\boldsymbol{\tau}}_1\widehat{\boldsymbol{\tau}}_2\Big), \quad (14)$$

where $V = -9.95$, $V_\sigma = 2.88$, $V_T = -1.47$, $V_\tau = 5.90$, $V_{\tau\sigma} = 4.91$, $V_{\tau T} = 1.51$ (all in MeV) and $r_0 = 1.8$ fm.

The second approach is to use experimental energies of the particle-particle (hole-hole) and particle-hole multiplets in odd-odd $(Z\pm1, N\pm1)$ and $(Z\pm1, N\mp1)$ nuclei, neighbouring the magic nuclide (Z, N). For example, consider the case when the spectrum of the proton-neutron multiplet, which is built on the levels j_π and j_ν being the closest to the Fermi surface, is available in the $(Z+1, N+1)$ nuclei. Then using the arguments based on Koopmans' theorem and taking into account the residual interaction between the valence proton and neutron quasiparticles, one obtains the formula

$$V_J^{\text{p-p}}(j_\pi j_\nu) \;= B(Z+1,N)+B(Z,N+1) -B(Z,N)-B(Z+1,N+1)+E_{\text{exc}}^J(j_\pi j_\nu)\;, \quad (15)$$

where B are the ground-state binding energies, while E_{exc}^J is the corresponding excitation energy of the state with spin J belonging to the proton-neutron multiplet. In the same way in the $(Z-1, N+1)$ nuclei, if the energies of the lowest proton-neutron particle-hole multiplet are known from the experiment, we have the relation for the orbitals lying the most closely to the Fermi surface:

$$V_J^{\text{p-h}}(j_{\pi'}j_\nu) \;= B(Z-1,N)+B(Z,N+1) -B(Z,N)-B(Z-1,N+1)+E_{\text{exc}}^J(j_{\pi'}j_\nu)\;, \quad (16)$$

where the prime in $j_{\pi'}$ means that we consider the hole state. Note that the particle-particle matrix elements may be expressed through the particle-hole ones by using the inverse Pandya transformation:

$$V_I^{\text{p-p}}(j_1j_2) \;=\; -\sum_J(2J+1)\begin{Bmatrix} j_1 & j_2 & J \\ j_1 & j_2 & I\end{Bmatrix}V_J^{\text{p-h}}(j_1j_2)\,. \quad (17)$$

It is important that the "empirical" matrix elements defined by (15) and (16) are the effective ones and implicitly include the bulk of nuclear correlations. At the same time, formulae (15) and (16) may be easily generalized for the case of orbitals positioned further from the Fermi surface.

To summarize, in our calculations instead of B_n^i, we determine their variations, $\delta B_{\pi,\nu}^i$ for one type of nucleons, arising from the addition (or removal) of nucleons of the other type. Thus, the B_n^i values are determined up to a constant term, which is the same for all members of a chain of isotopes (or isotones).

5 Results of the calculations

Figure 1 shows the experimental [13] and calculated proton separation energies in the $Z = 83$ isotopes as a function of neutron excess above the closed shell at $N = 126$ within the interval of $(N-Z)$ from -12 to $+4$. The calculations, performed here, were carried out by using interaction (14), with normalization to the ^{209}Bi nucleus. Different theoretical schemes, together with the experiment for

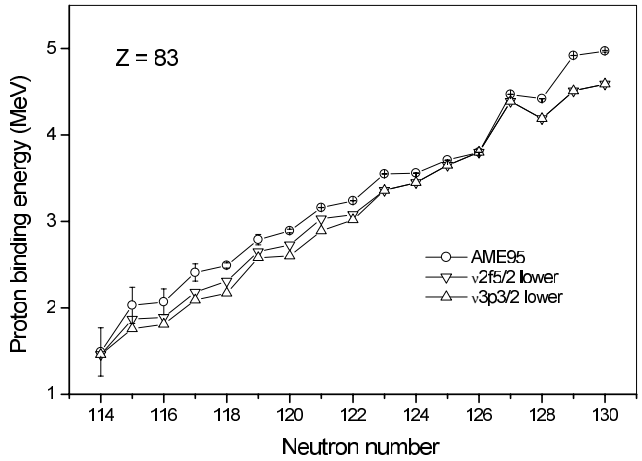

Fig. 1. Proton binding energies for the chain of isotopes with $Z = 83$. Open circles (AME95) present empirical data from the Atomic Mass Evaluation-95 [13]. Triangles show results of our calculations performed with the "standard" interaction (14) and correspond to different variants of the relative disposition of the neutron $3p_{3/2}$ and $2f_{5/2}$ orbits in the neutron-deficient isotopes of Bi.

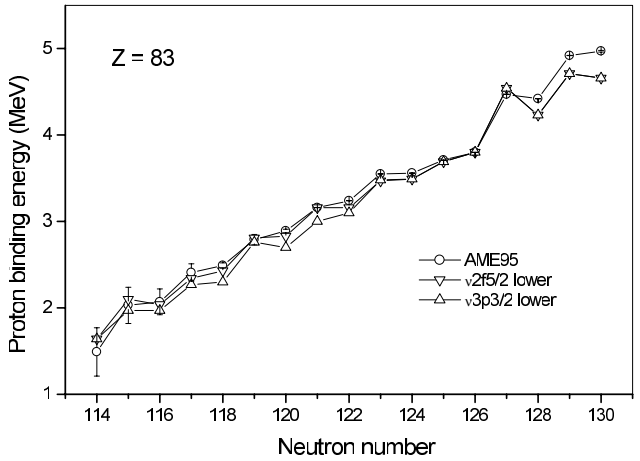

Fig. 2. The same as in fig. 1, but with the interaction from the work [16].

^{209}Bi, manifest that the proton is in the $1h_{9/2}$ state, while using the spectra and binding energies of the ^{207}Pb and ^{209}Pb nuclei neighbouring to ^{208}Pb, one obtains the energies of the neutron $3p_{3/2}$, $2f_{5/2}$, $3p_{1/2}$ and $2g_{9/2}$ states equal to -8.27, -7.94, -7.37 and -3.94 MeV, respectively. Experimentally the $3p_{3/2}$ and $2f_{5/2}$ levels are close to each other, thus a small variation of the neutron number N may cause their sequence to be interchanged. Consequently in fig. 1 we illustrate two variants of calculations: the first one when in nuclei with N substantially smaller than 126 we take as the lowest one the $3p_{3/2}$ state (as in ^{207}Pb), and the second one for the case when the neutron $2f_{5/2}$ state is lower than the $3p_{3/2}$ one. One can see that the second variant gives us better agreement with the experiment. The lowering of the $2f_{5/2}$ level below $3p_{3/2}$ with the decrease of N is also confirmed by the other data. For example, in $^{198}_{83}\mathrm{Bi}_{115}$ and $^{196}_{83}\mathrm{Bi}_{113}$, one can see [14] the low-lying 7^+ isomers with the extremely low energy in the case of $^{198}_{83}\mathrm{Bi}_{115}$. These isomers belong to the $\{\pi\, 1h_{9/2}, \overline{\nu\, 2f_{5/2}}\}$ configuration, which evidently is the lowest one in these odd-odd nuclei. Moreover, the interchange of the sequence of the aforementioned states is in agreement with the ideas presented in ref. [15]. Namely, the decrease of the average neutron spin-orbit potential in $(Z < N)$ nuclei with smaller N at fixed Z leads in our case (in comparison to ^{207}Pb) to a *relative* lowering of the neutron $2f_{5/2}$ orbital and to a *relative* raising of the $3p_{3/2}$ orbital.

In order to compare the present results with those obtained by using other residual interaction we have performed calculations with the effective forces determined in [16]. The latter interaction was obtained by the 12-parameter fitting to the values of the "empirical" pair matrix elements $V_J(j_1 j_2)$ derived from the experimental data by using the ansatz represented by formulae (15) and (16), both for odd-odd and even-even nuclei adjacent to magic nuclei near the stability line. This interaction represents a superposition of the Yukawa-type attractive and repulsive central components (long-range repulsion was included for a better description of the $T = 1$ two-quasiparticle states) with different radii, r_{01} and r_{02} (we used the parameter set with $r_{01} = 1.415$ fm and $r_{02} = 2.0$ fm), and includes also tensor and spin-orbit forces with $r_0 = 1.415$ fm, that corresponds to the π-meson mass. Since the contribution of spin-orbit components to the interaction from [16] is rather vague, the values of corresponding parameters are small and comparable with their uncertainties (especially for the triplet-even states), we have omitted the spin-orbit terms in this interaction. Our test calculations reveal only a small contribution of spin-orbit component to the total interaction [16]. Note that the main effect of the spin-orbit forces is to cause the formation of the mean-field spin-orbit splitting rather than two-quasiparticle multiplet splitting. We have to mention here that, according to [17], the radius of the spin-orbit interaction is much smaller than it was adopted in [16]. On the microscopical level this has a natural explanation as the aforementioned two-body force is conditioned by the exchange of heavier mesons. The results of corresponding calculations are shown in fig. 2. One can easily see from figs. 1 and 2 that the results of both calculations are similar.

Figure 3 illustrates the systematics of neutron separation energies in isotones with $N = 127$ (valence neutron in a $2g_{9/2}$ state); the empirical data [13] are compared to the results of our three calculations. The first calculation was carried out with the "empirical" matrix elements, obtained by applying relations (15) and (16) and by using the excitation energies of ^{210}Bi (multiplet $\{\nu 2g_{9/2}, \pi 1h_{9/2}\}$) and ^{208}Tl (multiplet $\{\nu 2g_{9/2}, \overline{\pi 3s_{1/2}}\}$). The calculations, normalized to the neutron separation energy of ^{209}Pb, show an excellent agreement with the experiment. The other calculation is performed by using interaction (14). Here one can see a good qualitative agreement with the experiment, including a reproduction of the irregularity at $(Z - 82) = 1$, but the slope of the curve is a little smaller

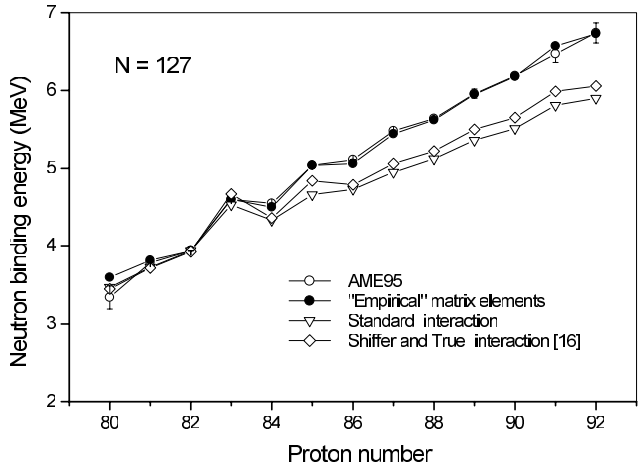

Fig. 3. Neutron binding energies for the $N = 127$ isotones. The data taken from the Atomic Mass Evaluation-95 [13] are shown by open circles, while the results of calculations using the "empirical" matrix elements as defined by ansätze (15) and (16) are indicated by filled circles. Calculations using the "standard" interaction (14) and the interaction from [16] are shown by open triangles and open diamonds, correspondingly.

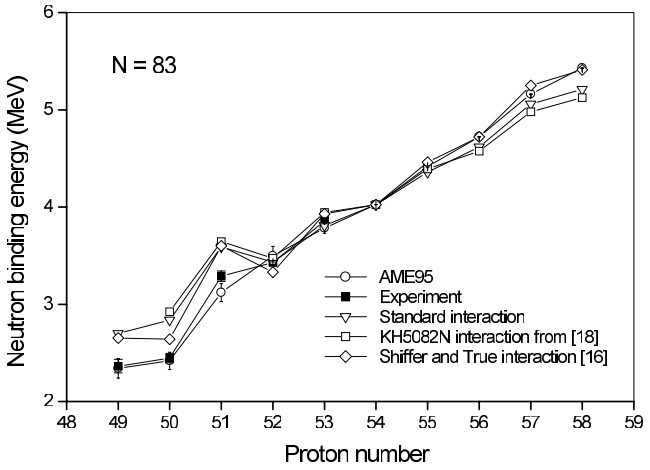

Fig. 4. Neutron binding energies in nuclei close to ^{132}Sn. Solid boxes show experimental values of the separation energies [19], while open circles are the data of systematics [13]. The triangles stand for the results of calculations that use the interaction (14), while open boxes show the calculations with the KH5082N interaction [18]. Results of calculations that use the interaction from [16] are marked by open diamonds.

than in the experiment. We also note that the two-body interaction [16] that was defined for the description of two-quasiparticle states in the "diagonal" scheme (we used this scheme also to determine the separation energies, see the discussion above) shows slightly better results than the "standard" interaction determined in the framework of the diagonalization procedure.

The calculated neutron separation energies for isotones with $N = 83$ close to ^{132}Sn are illustrated by fig. 4. The theoretical results are normalized to the value of B_ν for the isotone with $(Z - 50) = 4$, where the experimental uncertainty is small. In parallel to the matrix elements

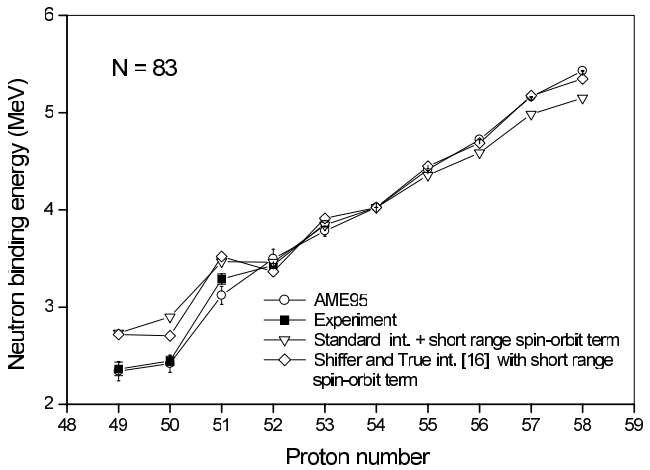

Fig. 5. The same as in fig. 4, but with the addition of the short-range two-body spin-orbit component into the interaction.

obtained by using the two-body interaction (14) we employed corresponding matrix elements for the configuration $\{\nu 2f_{7/2}, \pi 1g_{7/2}\}$ calculated in the framework of the G-matrix approach based on the Bonn A two-body interaction (KH5082N effective forces, see [18]), as well as the matrix elements that correspond to the two-body interaction [16]. As is seen in fig. 4, the most striking disagreement between the calculations and the data of systematics [13] is the absence in the latter of any irregularity at $(Z - 50) = 1$, observed at $(Z - 82) = 1$ in fig. 3. However, one should mention that recent experimental results on the values of neutron separation energies in the ^{132}In, ^{133}Sn and the ^{134}Sb nuclei obtained from the mass values [19] and our preliminary experimental values for neutron binding energies in ^{135}Te and ^{136}I have much better agreement with the results of our calculations, see fig. 4. Recall that the ^{132}Sn and ^{208}Pb nuclei are in some respect "twin" systems having similar shell structures and properties, since the quantum numbers of most of the single-particle orbitals relate simply as $n \to n$, $\ell \to \ell + 1$, $j \to j + 1$ [20]. Unfortunately, at the present time there is no sufficient experimental information on the $\{\nu 2f_{7/2}, \pi 1g_{9/2}\}$ configuration in ^{134}Sb, thus we could not perform calculations using the "empirical" matrix elements for the case of $N = 83$.

We have also calculated neutron separation energies for the $N = 83$ isotones using the "standard" interaction (14) with an addition of the short-range two-body spin-orbit term that was determined in [17] from a proper description of the mean-field spin-orbit splitting in light nuclei. It has the form

$$\widehat{\vartheta}_{ls}(1,2) = V_{LS} \cdot \exp\left(-\frac{r_{12}^2}{r_{0ls}^2}\right) \widehat{\boldsymbol{L}}_{12} \left(\widehat{\boldsymbol{s}}_1 + \widehat{\boldsymbol{s}}_2\right);$$

$$\widehat{\boldsymbol{L}}_{12} = \frac{1}{2} \left(\boldsymbol{r}_1 - \boldsymbol{r}_2\right) \times \left(\widehat{\boldsymbol{p}}_1 - \widehat{\boldsymbol{p}}_2\right), \qquad (18)$$

where $r_{0ls} = 1.0$ fm and $V_{LS} = -80$ MeV. This interaction is the same in triplet-even and triplet-odd states, but, due to the Pauli principle and to its short range, only the triplet-odd states contribute in practice to the

Table 1. Single-particle energies in ^{78}Ni corresponding to the potential (18). "Var 1" is the "Set 3" for ^{208}Pb taken from [15] with $V_0 = -51.99$ MeV, $V_{\ell s} \cdot r_{00}^2 = 32.70\,\mathrm{MeV} \cdot \mathrm{fm}^2$, $\beta = 1.36$, $\beta_{\ell s} = -0.6$, $r_{00} = 1.27\,\mathrm{fm}$, $r_{0c} = 1.25\,\mathrm{fm}$, $a(p) = 0.73\,\mathrm{fm}$, $a(n) = 0.72\,\mathrm{fm}$. "Var 2" is the "Set 2" taken from [15] (it was also used in [12] for the description of the mass surface of nuclei close to ^{78}Ni) with $V_0 = -51.5$ MeV, $V_{\ell s} \cdot r_{00}^2 = 35.7\,\mathrm{MeV} \cdot \mathrm{fm}^2$, $\beta = \beta_{\ell s} = 1.39$, $r_{00} = 1.27\,\mathrm{fm}$, $r_{0c} = 1.25\,\mathrm{fm}$, $a(p) = 0.67\,\mathrm{fm}$, $a(n) = 0.55\,\mathrm{fm}$. "Var 3" is the same as "Var 1", but with $V_{\ell s} \cdot r_{00}^2 = 36.0\,\mathrm{MeV} \cdot \mathrm{fm}^2$ and $\beta = 1.42$.

$\pi\, n\ell j$	Var 1	Var 2	Var 3	$\nu\, n\ell j$	Var 1	Var 2	Var 3
$\pi\, 1s1/2$	−42.73	−42.85	−43.14	$\nu\, 1s1/2$	−34.15	−34.45	−33.73
$\pi\, 1p3/2$	−35.67	−36.12	−36.10	$\nu\, 1p3/2$	−27.67	−28.21	−27.33
$\pi\, 1p1/2$	−34.56	−34.62	−34.88	$\nu\, 1p1/2$	−26.25	−27.19	−25.75
$\pi\, 1d5/2$	−27.64	−28.46	−28.10	$\nu\, 1d5/2$	−20.54	−21.10	−20.31
$\pi\, 1d3/2$	−25.21	−25.08	−25.44	$\nu\, 1d3/2$	−17.41	−18.69	−16.85
$\pi\, 2s1/2$	−24.20	−24.38	−24.56	$\nu\, 2s1/2$	−17.40	−17.70	−17.05
$\pi\, 1f7/2$	−18.87	−20.08	−19.39	$\nu\, 1f7/2$	−12.94	−13.34	−12.85
$\pi\, 1f5/2$	−14.77	−14.27	−14.88	$\nu\, 2p3/2$	−9.29	−9.02	−9.04
$\pi\, 2p3/2$	−14.59	−14.86	−14.97	$\nu\, 1f5/2$	−7.74	−9.07	−7.11
$\pi\, 2p1/2$	−13.07	−12.67	−13.29	$\nu\, 2p1/2$	−7.49	−7.46	−7.07
$\pi\, 1g9/2$	−9.56	−11.16	−10.14	$\nu\, 1g9/2$	−5.02	−5.11	−5.08
$\pi\, 1g7/2$	−3.60	−2.53	−3.58	$\nu\, 2d5/2$	−1.93	−1.07	−1.81
				$\nu\, 3s1/2$	−1.14	−0.39	−0.99
				$\nu\, 2d3/2$	0.30	0.82	0.54
				$\nu\, 1g7/2$	2.06	1.16	2.68
				$\nu\, 1h11/2$	2.94	3.34	2.76

spin-orbit splitting providing its proper isospin dependence (see [15]). The short-range spin-orbit interaction (18) was substituted for the long-range spin-orbit term in the interaction from [16]. The results of such calculations are illustrated in fig. 5. A comparison of fig. 4 and fig. 5 shows that the spin-orbit term does not essentially change the results of our calculations.

Concluding this section, we present the results on separation energies in the third region of nuclides —the region of the utmost neutron-rich nuclei in the vicinity of ^{78}Ni, lying on the path of the astrophysical r-process. We note here, that the calculations of single-particle spectra performed by using the phenomenological potential reveal a close disposition of the proton single-particle orbits $2p_{3/2}$ and $1f_{5/2}$ in this region of the nuclidic chart. Table 1 lists the calculated results on the single-particle proton and neutron energies in ^{78}Ni using different sets of parameters for the potential

$$U(r,\hat{\sigma}) = \frac{U_0}{1+\exp[(r-R)/a]} + U_{\ell s} r_{00}^2 \frac{1}{r}\frac{\mathrm{d}}{\mathrm{d}r}\left[\frac{1}{1+\exp[(r-R)/a]}\right]\widehat{\boldsymbol{\ell}}\cdot\widehat{\boldsymbol{s}}, \quad (19)$$

where $U_0 = V_0(1+\frac{1}{2}\beta\frac{N-Z}{A}\tau_3)$, $U_{\ell s} = V_{\ell s}(1+\frac{1}{2}\beta_{\ell s}\frac{N-Z}{A}\tau_3)$, $R = r_{00}A^{1/3}$, $\tau_3 = 1$ for protons and $\tau_3 = -1$ for neutrons (for protons the potential of a uniformly charged sphere with the radius $R_c = r_{0c}A^{1/3}$ has been added).

One can see from table 1 that the sequence of the proton $2p_{3/2}$ and $1f_{5/2}$ orbitals can be interchanged by a small variation of parameters entering eq. (19). Consequently, we made self-consistent Hartree-Fock calculations using the Skyrme III interaction, the results are shown in table 2. These calculations were performed by including (variant SIII-1) and omitting (variant SIII-2) spin density terms contributing to the spin-orbit splitting, while the Coulomb exchange terms were treated in the Slater approximation. The proton and neutron densities in ^{78}Ni, corresponding to the SIII-1 calculation are presented in fig. 6. One can see that the neutron mean square-root radius in ^{78}Ni ($r_n = 4.206$ fm) is considerably larger than the proton one ($r_p = 3.962$ fm). We have also calculated the total binding energy B_{tot} of 642.2 MeV in ^{78}Ni, which should be compared to the empirical total binding energy of 641.4 (1.1) MeV derived from the systematics [13]. The analogous densities for ^{56}Ni are illustrated by fig. 7.

Table 2. Single-particle energies in ^{78}Ni from self-consistent calculations.

$\pi\, n\ell j$	SIII-1	SIII-2	$\nu\, n\ell j$	SIII-1	SIII-2
$\pi\, 1d5/2$	−30.70	−30.95	$\nu\, 1d5/2$	−26.60	−26.88
$\pi\, 1d3/2$	−27.99	−27.52	$\nu\, 1d3/2$	−23.88	−23.44
$\pi\, 2s1/2$	−25.82	−25.74	$\nu\, 2s1/2$	−21.68	−21.58
$\pi\, 1f7/2$	−20.20	−20.55	$\nu\, 1f7/2$	−16.17	−16.64
$\pi\, 1f5/2$	−15.11	−14.50	$\nu\, 1f5/2$	−11.07	−10.36
$\pi\, 2p3/2$	−14.05	−14.03	$\nu\, 2p3/2$	−10.73	−10.70
$\pi\, 2p1/2$	−12.64	−12.46	$\nu\, 2p1/2$	−9.06	−8.89
$\pi\, 1g9/2$	−9.29	−9.68	$\nu\, 1g9/2$	−5.71	−6.29
			$\nu\, 2d5/2$	−1.01	−1.04
			$\nu\, 3s1/2$	−0.28	−0.25
			$\nu\, 2d3/2$	0.54	0.64
			$\nu\, 1g7/2$	1.55	2.30

The proton $2p_{3/2}$ and $1f_{5/2}$ orbitals are close to each other and their mutual separation may be changed by a small variation of the parameters. At the same time, the experimental data on the single-particle spectra in nuclei close to ^{78}Ni are not available yet. Therefore in fig. 8 we present the B_ν values calculated using interaction (14) and making two assumptions on the sequence of the $2p_{3/2}$ and

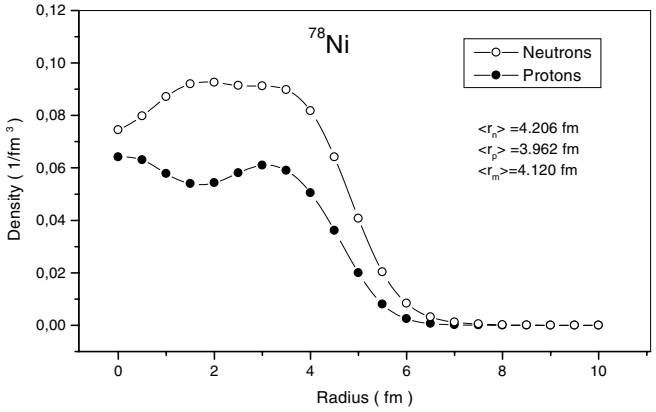

Fig. 6. Proton and neutron densities in ^{78}Ni.

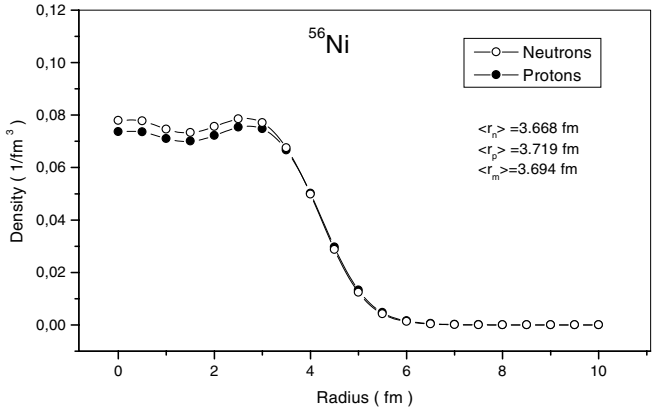

Fig. 7. Proton and neutron densities in ^{56}Ni.

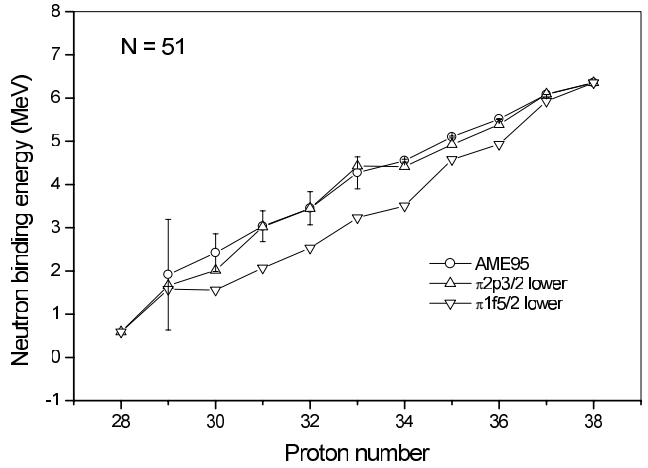

Fig. 8. Neutron binding energies for the $N = 51$ isotones close to ^{78}Ni. Open circles (AME95) show the empirical data [13], while triangles are the results of calculations performed by using the "standard" interaction (14) and corresponding to different variants of the relative disposition of the proton $2p_{3/2}$ and $1f_{5/2}$ orbits in nuclei close to ^{78}Ni.

$1f_{5/2}$ orbitals. A good agreement with the experiment is obtained in the case when the proton state $2p_{3/2}$ is the lower one. This conclusion is also valid if we include the

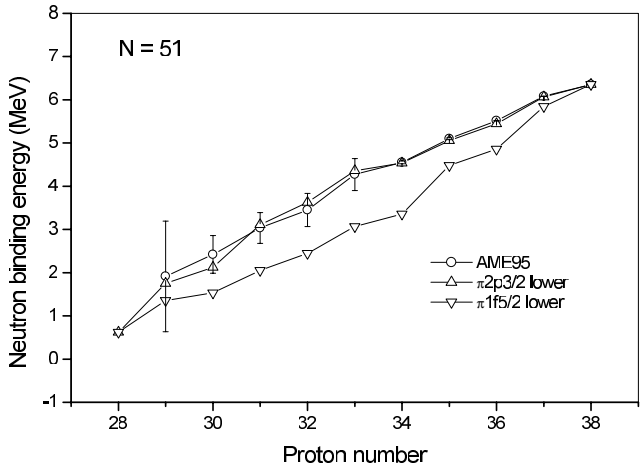

Fig. 9. The same as in fig. 8, but with the addition of the short-range spin-orbit term to interaction (14).

short-range spin-orbit term in the interaction (see fig. 9). Thus, the information on the neutron separation energies in the chain of isotones with $N = 51$ allows us to get a conclusion on the characteristics of single-particle spectra in the region of ^{78}Ni.

6 Conclusion

In this paper we propose a new method for the calculation of one-nucleon separation energies in the chains of isotopes or isotones. This method is based on the multiparticle shell model and may be successfully applied for spherical nuclei not far from the closed shells. We demonstrate a good agreement with the experiment for proton binding energies in the chain of isotopes with $Z = 83$ and for neutron binding energies in the chain of isotones with $N = 127$. At the same time, the obtained disagreement with the existing systematics [13] concerning the neutron binding energies in the chain of isotones at $N = 83$ may stimulate more detailed experimental studies of these nuclear characteristics. In fact, the latest experimental data [19] as well as the results of recent calculations [21] based on the other approach also demonstrate the existence of the staggering effect in neutron binding energies for the isotones with $N = 83$. Our calculations based on the multiparticle shell model manifest the value of the neutron separation energy in ^{79}Ni of about 0.65 MeV. This magnitude is smaller than that of the neutron binding energy in ^{79}Ni obtained in single-particle calculations (the average value of the $B_\nu^{2d5/2}$ is about 1.3 MeV, see tables 1 and 2). However, the magnitude of the neutron binding energy in ^{79}Ni obtained in our paper by using the multiparticle shell model is rather close to the value $B_\nu = 0.52$ MeV for ^{79}Ni from ref. [21]. At the same time, one should mention that it would be more correct to identify the neutron separation energy not with the single-particle energy of the upper neutron (with the inverse sign), but rather with the difference of the binding energies of the corresponding neighbouring nuclei that differ by one neutron.

Calculating the values of the binding energies of ^{79}Ni and ^{78}Ni in the framework of the Hartree-Fock method, we obtain the value of B_ν in ^{79}Ni equal to ~ 0.8 MeV, that is also a bit smaller than the value obtained from the single-particle spectra, see table 2. So, the value of B_ν in ^{79}Ni of about 0.65 MeV obtained by using the multiparticle shell model seems to be reasonable.

This work was performed under the support of the Russian Foundation for Basic Research (project No. RSGSS-1124.2003.2).

References

1. T.H. Koopmans, Physica **1**, 104 (1933).
2. B.F. Bayman, A. Lande, Nucl. Phys. **77**, 11 (1966).
3. I. Talmi, A. de Shalit, *Nuclear Shell Theory* (Academic Press, Inc., N.Y., 1963).
4. S.P. Pandya, Phys. Rev. **103**, 256 (1956).
5. L.A. Sliv, Yu.I. Kharitonov, in *Spectroscopic and Group Theoretical Methods in Physics* (North-Holland, Amsterdam, 1968) p. 275.
6. V.I. Isakov, S.A. Artamonov, L.A. Sliv, Bull. Acad. Sci. USSR, Phys. Ser. **41**, 72 (1977).
7. S.A. Artamonov, V.I. Isakov, S.G. Kadmensky, I.A. Lomachenkov, V.I. Furman, Sov. J. Nucl. Phys. **36**, 486 (1982).
8. K.I. Erokhina, V.I. Isakov, Phys. At. Nucl. **57**, 198 (1994).
9. K.I. Erokhina, V.I. Isakov, Phys. At. Nucl. **59**, 589 (1996).
10. V.I. Isakov, K.I. Erokhina, Phys. At. Nucl. **65**, 1431 (2002).
11. V.I. Isakov, K.I. Erokhina, B. Fogelberg, Yu.N. Novikov, H. Mach, K.A. Mezilev, Part. Nucl., Lett. **5[102]**, 44 (2000).
12. V.I. Isakov, K.A. Mezilev, Yu.N. Novikov, K.I. Erokhina, B. Fogelberg, H. Mach, Phys. At. Nucl. **63**, 1740 (2000).
13. G. Audi, A.H. Wapstra, Nucl. Phys. A **595**, 409 (1995); `http://www-nds.iaea.or.at/ndspub/masses/`.
14. M. Huyse, P. Decrock, P. Dendooven, G. Reusen, P. Van Duppen, J. Wauters, Phys. Rev. C **46**, 1209 (1992).
15. V.I. Isakov, K.I. Erokhina, H. Mach, M. Sanchez-Vega, B. Fogelberg, Eur. Phys. J. A **14**, 29 (2002).
16. J.P. Shiffer, W.W. True, Rev. Mod. Phys. **48**, 191 (1976).
17. V.N. Guman, L.A. Sliv, Yu.I. Kharitonov, Sov. J. Nucl. Phys. **10**, 302 (1970).
18. A. Korgul, H. Mach, B. Fogelberg, W. Urban, W. Kurcewicz, T. Rzaca-Urban, P. Hoff, H. Gausemel, J. Galy, J.L. Durell, W.R. Phillips, A.G. Smith, B.L. Valery, N. Schulz, I. Ahmad, L.R. Morrs, M. Górska, V.I. Isakov, K.I. Erokhina, J. Blomqvist, F. Andreozzi, F. Corragio, A. Covello, A. Gargano, Eur. Phys. J. A **15**, 181 (2002).
19. B. Fogelberg, K.A. Mezilev, H. Mach, V.I. Isakov, J. Slivova, Phys. Rev. Lett. **82**, 1823 (1999).
20. J. Blomqvist, in *Proceedings of the 4th International Conference on Nuclei Far from Stability, Helsingor, Denmark, 7-13 June, 1981*, CERN Report 81-09 (CERN, Geneva, 1981) p. 536.
21. P. Möller, J.R. Nix, W.D. Myers, W.J. Swiatecki, At. Data Nucl. Data Tables **59**, 185 (1995).